



## INVITED PAPER

# The Scaling of Olfaction: Moths have Relatively More Olfactory Surface Area than Mammals

Nina Mohebbi<sup>\*2</sup>, Andrew Schulz<sup>ID\*2</sup>, Thomas L. Spencer<sup>\*</sup>, Kelsie Pos<sup>†</sup>, Andrew Mandel<sup>ID\*</sup>, Jérôme Casas<sup>‡</sup> and David L. Hu<sup>ID\*§,1</sup>

<sup>\*</sup>George W. Woodruff School of Mechanical Engineering, Georgia Institute of Technology, Atlanta, GA 30332, USA; <sup>†</sup>School of Biological Sciences, George Washington University, Washington, DC 20052, USA; <sup>‡</sup>Institut de Recherche sur la Biologie de l’Insecte, CNRS, Université de Tours, Tours, UMR 7261, France; <sup>§</sup>School of Biological Sciences, Georgia Institute of Technology, Atlanta, GA 30332, USA

<sup>1</sup>E-mail: [hu@me.gatech.edu](mailto:hu@me.gatech.edu)

<sup>2</sup>indicates co-first author

**Synopsis** Body size affects nearly every aspect of locomotion and sensing, but little is known of its influence on olfaction. One reason for this missing link is that olfaction differs fundamentally from vision and hearing in that molecules are advected by fluid before depositing on olfactory sensors. This critical role of fluid flow in olfaction leads to complexities and trade-offs. For example, a greater density of hairs and sensory neurons may lead to greater collection, but can also lead to reduced flow through hairs and additional weight and drag due to a larger olfactory organ. In this study, we report the surface area and sensory neuron density in olfactory organs of 95 species of moths and mammals. We find that approximately 12–14% of an olfactory system’s surface area is devoted to chemosensors. Furthermore, total olfactory surface area and olfactory sensing surface area scale with body mass to the 0.49 and 0.38 powers, respectively, indicating that moths have a higher proportion of olfactory surface area than mammals. The density of olfactory neurons appears to be near the limit, at 10,000 to 100,000 neurons per square mm across both insects and mammals. This study demonstrates the need for future work detailing how the scaling of olfaction and other senses vary across taxa.

## Introduction

The need to escape predators, find mates, and detect prey has pushed the envelope for speed and sensitivity in odor detection. Consequently, olfaction is an essential process for organisms ranging from bacteria (Nijland and Burgess 2010) to the largest vertebrates. While much work has been done on the neuroscience of olfaction, little is known of universal principles that span body size. Allometric relationships have been found for the eye and other sensory organs (Howland et al. 2004; Nummela 1995), but not for olfactory organs. Understanding the scaling of olfaction will help build a more complete picture for how life changes as a function of body size and may help with the design of bio-inspired chemical sensors.

In this study, we focus on two aspects of olfaction, the surface area and neuronal density of the olfactory organ. Olfaction works by the advection, diffusion, and

eventual deposition of olfactory chemicals directly onto a sensing surface (Wyatt 2009). While the deposition of chemicals is subject to molecular forces, we may gain some insight by considering the deposition of particles. The rate,  $\frac{dN}{dt}$ , of particles collected by an object in flow may be written as

$$\frac{dN}{dt} = \eta CUA \quad (1)$$

where  $\eta$  is the efficiency of collection,  $C$  is the concentration of particles in the air (e.g., number of particles per cubic meter),  $U$  is the air velocity, and  $A$  is the object’s cross-sectional area normal to the flow. While the concentration  $C$  is outside the animal’s control, all other variables ( $U$ ,  $A$ ,  $\eta$ ) can be exploited by animals to maximize particle capture. For example, airspeed can be increased by inhala-

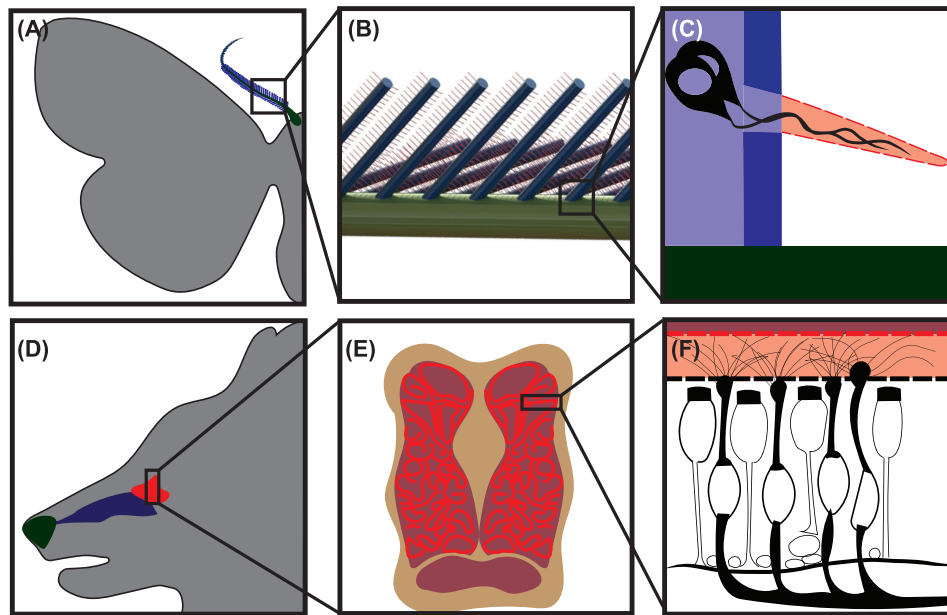


**Fig. 1** Olfactory organs of moths and mammals. **(A)** A moth antenna with two levels of magnification. The antenna stalk is green, branches are blue, and sensilla are red. **(B)** The antenna stalk surface. **(C)** A single sensillum extrudes from a branch. The receptor cells and their dendrites are shown in black. Dashed surface of sensillum represent pores. Sensillum lymph shown in light red shading. **(D)** A dog's nasal cavity with naris in green, maxilloturbinate region in blue, and ethmoturbinate (sensing) region in red. **(E)** A cross section of the ethmoturbinate region. The cross section faces the nostril. Airflow travels into the page. **(F)** Cilia and olfactory cells are in black. The mucus lining of the ethmoturbinate region is in light red. The mucous-air interface is the dashed red line and the mucus-olfactory-epithelium interface is the black dashed line. Drawing modified from McEwen (McEwen et al. 2008). Illustrations done by A. Schulz.

tion, sniffing, flying into an odor plume, or waiting for passing winds to bring in molecules. In this study, we focus specifically on the scaling of olfactory organ.

Measuring the sensing surface area of the eye and tongue is easier than measuring the sensing surface area for olfaction. This difficulty arises because the olfactory organs of insects and mammals are complex three-dimensional shapes that affect fluid flows and increase the chances of odor capture (Cheer and Koehl 1987). One difficulty in measuring mammal olfaction is that mammals keep their olfaction sensors protected inside the nose. Air passes through the naris, then the maxilloturbinate, and finally the ethmoturbinate region (Fig. 1D). The walls of the ethmoturbinate region, which make up the olfactory epithelium, are intricately shaped (Fig. 1E). The olfactory epithelium contains olfactory sensory neurons and their projecting cilia, both of which are covered by a mucus layer (Fig. 1F) (Buck 2000; Kandel et al. 2000). The total surface area of the olfactory organ will often be larger than the fragile area containing sensing neurons, which we refer to as the sensing surface area. In this work, we will seek to measure the sensing proportion, the ratio of the sensing surface area to the total surface area of the olfactory organ.

We choose to focus on the sensing proportion because we hypothesize that a more effective olfactory system would have a greater proportion of sensing surface area. However, olfactory organs are multi-purpose and feature prominent non-sensing zones as well. Thus we do not expect the sensing proportion to approach one. Examples of these additional olfactory organ roles include heating and moisturizing air in the mammalian nose and providing structural support in the plumose moth antenna. Furthermore, olfactory organs may have aerodynamic features that improve the efficiency of capture through fluid mechanical focusing (Spencer et al. 2020). We also note that there is a longstanding debate whether the acuity of olfaction should be related to the number of neurons or the proportion of an olfactory organ's surface area to body surface area (Smith and Bhatnagar 2004).

A larger sensing surface area should improve the chances that an odor molecule deposits onto a sensing surface. To further understand olfaction in this study, we report the density of sensors. For animals, these sensors are olfactory sensory neurons (OSNs), and the chance of detection improves with a higher density of OSNs. Olfactory sensory neurons, which are found in mammalian olfactory epithelium, insect antennae, and insect feet, enable the olfactory system to inter-

act directly with its surroundings by expressing receptors sensitive to both chemical and mechanical stimuli (Grosmaître et al. 2007). OSN axons rapidly transmit odorant information upon activation, as they innervate an insect's antennal lobe and a mammal's olfactory bulb (Sachse and Krieger 2011).

In this study, we simply counted olfactory sensor neurons within sensory zones. This is a first-order approach, and we note that there is hidden complexity within the neurons themselves that we will not attempt to measure. For example, a human olfactory system has 6–10 million OSNs, with each OSN extending dendrites to form an olfactory knob (Sankaran et al. 2012). Each knob in turn has 5–50 cylindrical cilia, each with a diameter of 0.25–0.5 microns and length of 30–200 microns, which extend into the mucus of the olfactory epithelium. Assuming 6 million OSNs with 25 cilia each (each cilium of diameter 0.5 microns and length 30 microns) results in a surface area of 71 cm<sup>2</sup> for the olfactory cilia alone (Sankaran et al. 2012). This additional surface area is especially extraordinary when considering that the total surface area of the human olfactory epithelium is only 10 cm<sup>2</sup> (Purves et al. 2001). Before such in-depth calculations can be done for other animals, we must first ascertain the surface area of the olfactory organ.

## Methods

### Surface area

Both antenna and nasal cavities come in pairs, but for simplicity we report the surface area of a single antenna and a single nasal cavity. The estimated total surface area of a single moth antenna was calculated according to  $A = \pi(L_{st}d_{st} + N_bL_b d_b + N_s N_s L_s d_s)$  where  $L_{st}$  is the length of one stalk,  $d_{st}$  is the stalk diameter,  $N_b$  is the number of branches on one stalk,  $L_b$  is the length of one branch,  $d_b$  is the branch diameter,  $N_s$  is the number of sensilla on one branch,  $L_s$  is the length of one sensillum, and  $d_s$  is the sensillum diameter. The total number of branches and sensilla were not individually counted but rather estimated using the center to center spacing. On each antenna stalk, there are two branch arrays, and on each branch array, sensilla are found in pairs. All moth surface area measurements were completed using ImageJ image processing (Schneider et al. 2012).

### Olfactory sensory neuron density

Insect antenna stalks are modeled as cylinders, with the estimated surface area of one stalk calculated according to  $A_{stalk} = \pi L_{st} d_{st}$  where  $L_{st}$  is the length of one stalk and  $d_{st}$  is the stalk diameter. In the calculation of sen-

sory neuron density, we considered the stalk alone and neglected the branches and sensilla.

To estimate OSN density for mammals, we measure the olfactory epithelium surface area in one nasal fossa. If surface area reported by previous investigators were for both nasal fossae, we divided this number by two to represent one nasal fossa. OSN counts are given for one antenna stalk for insects and for the olfactory epithelium in one nasal fossa for mammals. Insect OSN density is calculated by dividing the number of OSNs on one antenna stalk by the corresponding antenna stalk surface area. Mammal OSN density is calculated by dividing the number of OSNs in the olfactory epithelium of one nasal fossa by the corresponding olfactory epithelium surface area in one nasal fossa. Raw data was collected from 29 literature sources (Table S3).

### Phylogenetics comparison of species

We hypothesize that the power law trend for olfactory surface area is due to phylogenetic dependence of the species studied. To determine the extent that our trends are influenced by phylogenetic closeness within mammalian taxa, we calculated Phylogenetic Independent Contrasts (PIC). This is a statistical method that controls for the effects of phylogenetic closeness on our data (Martins and Hansen 1997). We began by generating a consensus phylogeny using the *consensus* function in the package *ape* in R studio from 500 pruned subsets from VertLife (<http://vertlife.org/phylosubsets>). We generated this consensus tree for the mammalian species studied to examine phylogenetic independent contrasts of turbinate and epithelium surface area (Figs. S1 and S2).

We found that mammal epithelium and body mass independent contrasts are not statistically related, and thus phylogenetic dependence may have a small influence on our trend ( $P=0.0626$ , Fig. S2). Using the same methodology, we found that the mammal turbinates and body mass independent contrasts were statistically related even with phylogeny accounted for ( $P=1.37e-08$ , Fig. S1). In conclusion, the total surface of mammals requires a greater number of more distantly related species to draw conclusions.

To determine if the observed trends for moths are influenced by phylogenetic closeness, we used Abouheif's  $C_{mean}$ , an autocorrelation index that tests for serial independence between trait values of neighboring species (Münkemüller et al. 2012; Abouheif 1999; Pavoine et al. 2008). We used phyloTv2 phylogeny generator using NCBI taxonomy and scientific names to generate our phylogeny. Because this generates a tree with no branch lengths, we used the function *abouheif.moran* and method *oriAbouheif* for the proximity matrix in the

adephylo package in R studio (Münkemüller et al. 2012; Abouheif 1999). Computing the  $C_{mean}$  of moth body mass, sensilla surface area, and total antenna surface area we find none are statistically correlated with neighboring species displaying statistical values of  $P=0.109$ ,  $P=0.664$ ,  $P=0.576$ , respectively. Therefore, we confirm that moth mass, sensilla surface area, and total antenna surface area are not correlated with neighboring species.

## Results

We collected  $N = 95$  olfactory surface area measurements across 51 species from studies of moth antennae (Spencer et al. 2020), nasal cavities of humans (Purves et al. 2001), and non-human mammals (Green et al. 2012; Yee et al. 2016; Smith et al. 2014). These studies all date after the year 2000, following the advent of CT-scanning for accurately measuring the nasal cavity size and shape.

We begin with the hypothesis that olfactory organs are isometric: their proportions do not change with body size. An animal of characteristic size  $L$  has a mass  $M$  that scales as  $L^3$  and a surface area that scales with  $L^2$ . Isometry thus suggests that the surface area of an animal's external sensory organs scales as  $M^{2/3}$  (Calder 1996; Schmidt-Nielsen and Knut 1984). While attractive for its simplicity, isometry fails to describe nearly all sensing modalities. For example, the eye surface area scales as  $M^{0.4}$  (for birds, reptiles, and fish,  $N = 292$ ) (Howland et al. 2004). This exponent is less than 0.66 and is defined as negative allometry. Thus, larger animals have proportionally smaller eyes than smaller animals. The reverse may be true for hearing because the middle ear's mass scales with  $M^{1.2}$  (Nummela 1995).

Fig. 2A shows the relationship between body mass and total surface area of the olfactory region, where body mass spans eight orders of magnitude, from  $10^{-5}$  to  $10^3$  kg. Total surface area for moths is defined as that of one antenna, and for mammals as that of one nasal fossa shown in Fig. 1D. Only a small fraction of the olfactory organ has sensory neurons. Fig. 2B shows the olfactory sensing surface area, defined as that of the sensilla for moths and the ethmoturbinate region for mammals (shown in red in Fig. 1A–F).

Approximating the stalk, branches, and sensilla of an antenna as cylinders, the average plumose moth antenna has a total surface area of  $26 \text{ mm}^2$ , the surface area of a thumbtack. For moths, the scaling for the total and sensing surface areas are  $S_{total, moth} = 2700M^{0.44}$  and  $S_{sensing, moth} = 330M^{0.34}$ , respectively. In mammals, the complex shape of the ethmoturbinate region greatly increases its surface area compared to the simple pipe used in artificial sensing systems (Spencer et al. 2021).

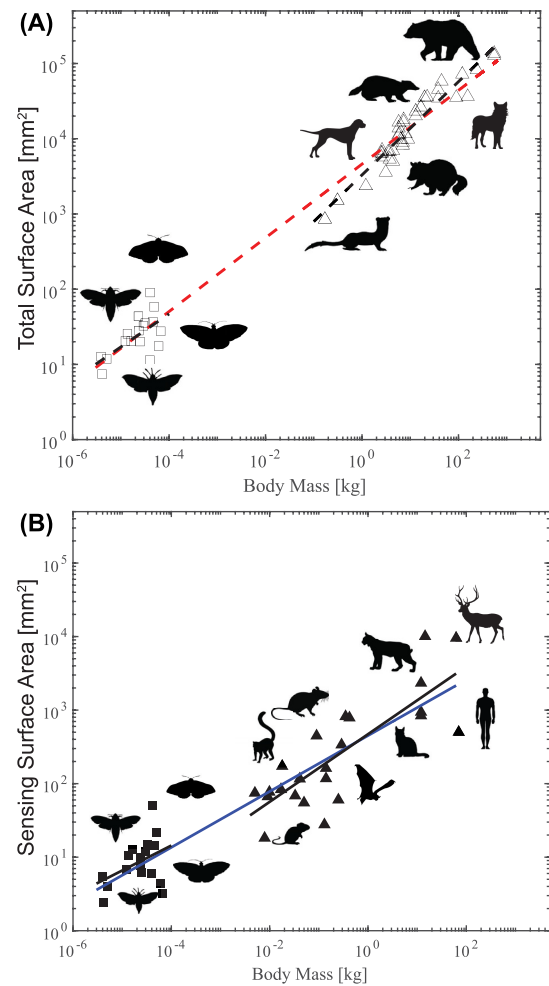


**Fig. 2** Olfactory scalings. **(A)** The relationship between total olfactory organ surface area ( $\text{mm}^2$ ) and body mass  $M$  (kg). Open squares represent surface area of one bi-pectinate moth antenna including stalk, branches, and sensilla. Open triangles represent olfactory turbinal surface area in one nasal fossa (Green et al. 2012). The black dashed lines show power fit laws for the moths and the mammals separately. The red dotted line shows the power law fit for all the animals together. Raw data shown in Table S1. Silhouettes from Adobe Stock photos. **(B)** Relation between olfactory sensing surface area ( $\text{mm}^2$ ) and body mass  $M$  (kg). Silhouettes from Adobe Stock photos. Raw data shown in Table S2. Filled squares represent surface area of sensilla from one antenna. Filled triangles represent olfactory epithelium surface area in one nasal fossa. The black lines show power fit laws for the moths and the mammals separately. The blue solid line shows the power law fits all the animals together. Silhouettes from Adobe Stock photos. Data for each measurement category was collected from the following literature sources: mass (Jumbo et al. 2010; Nijhout et al. 2006; Żółtowska et al. 2011; Mongeau et al. 2015; Koella and Lyimo 1996; Lindsey 2002; Gross et al. 1982; Abrams 2019; Hedberg 2007; Kobayashi et al. 2012; Xi et al. 2016; Meisami et al. 1990), surface area (Jacob et al. 2017; Symonds et al. 2012; Shields and Hildebrand 2001; Tsujiuchi et al. 2007; Lockey and Willis 2015; Vršanský and Wang 2017; Saltin et al. 2019; Garman 1921; Saager and Gewecke 1989; Gross et al. 1982; Horowitz et al. 2014; Moulton and Beidler 1967; Gasser 1956; Meisami et al. 1990; Smith et al. 2011).

**Table 1** Olfactory surface area and olfactory sensory neuron (OSN) density scalings. Body mass  $M$  is in kg. Surface areas in square mm.

Measurement	Variable	Best Fit	$R^2$	$N$	PIC	$C_{\text{mean}}$
Moth Antenna Total Surface Area	$S_{\text{total, moth}}$	$2700M^{0.44}$	0.39	17		0.576
Moth Sensilla Surface Area	$S_{\text{sensing, moth}}$	$330M^{0.34}$	0.17	17		0.664
Mammal Turbinates Total Surface Area	$S_{\text{total, mammal}}$	$3300M^{0.62}$	0.92	38	$1.37 \cdot 10^{-8}$	
Mammal Sensory Epithelium Surface Area	$S_{\text{sensing, mammal}}$	$470M^{0.46}$	0.67	23	0.063	
Aggregate Total Surface Area	$S_{\text{total, all}}$	$4600M^{0.49}$	0.98	55		
Aggregate Sensing Surface Area	$S_{\text{total, sensing}}$	$450M^{0.38}$	0.84	40		

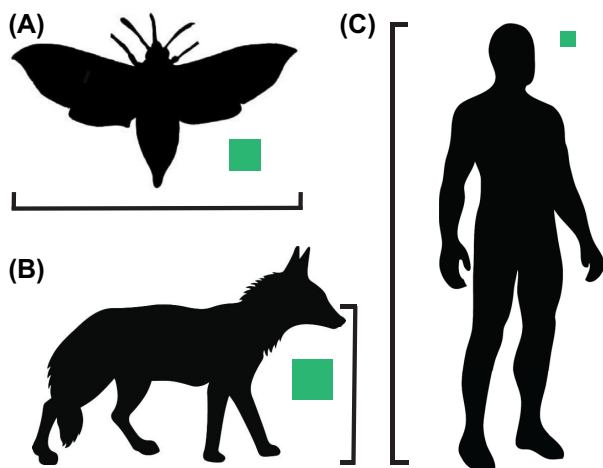


**Fig. 3** The scaling of olfactory sensing surface area with body size. **(A)** *Lymantria dispar* (gypsy moth): scale bar represents 28 mm wing span and green box represents the 50 mm<sup>2</sup> sensilla area (Spencer et al. 2020). **(B)** *Canis latrans* (coyote): scale bar represents 26 cm shoulder height and green box represents the 100 cm<sup>2</sup> olfactory surface area in one nasal fossa (Yee et al. 2016). **(C)** *Homo Sapiens* (human) scale bar represents 165 cm height and green box represents the 5 cm<sup>2</sup> olfactory epithelium surface area in one nasal fossa (Purves et al. 2001). Silhouettes from Adobe Stock photos. Raw data shown in Table S3.

In mammals, the total surface area scales as  $S_{\text{total, mammal}} = 3300M^{0.62}$  and the sensing surface area scales as  $S_{\text{sensing, mammal}} = 470M^{0.46}$ . The scalings for sensing and total surface areas are presented in Table 1. This result that sensing surface area increase with body size is at least qualitatively consistent with measurements of primates, which found that sensing length scale scales as  $M^{0.484}$  (Smith et al. 2007).

Grouping the moth sensilla and mammal epithelium measurements together gives an aggregate scaling for the sensing olfactory sensing surface area,  $S_{\text{sensing, all}} = 450M^{0.38}$  with  $R^2 = 0.84$ . Doing the same for total olfactory surface area yields  $S_{\text{total, all}} = 4600M^{0.49}$  with  $R^2 = 0.98$ . The high coefficient of determination for each of these aggregate scalings shows that power laws well describe the olfactory surface areas for both moths and mammals.

We define the sensing proportion as the ratio of the sensing surface area to the total surface area of the olfactory organ. Considering the pre-factors of the power law exponents in Table 1, the sensing proportion is 1:8 for insects and 1:7 for mammals. Thus, nearly 86–88% of the olfactory organ is not explicitly used for sensing. Since the animals considered span 8 orders of magnitude in body size, the proportion is highly conserved across body size. The sensing proportion reflects the costs of carrying around a larger olfactory organ than necessary. At least for moths, such an organ can accrue drag and require energetic costs to grow and maintain. The sensing proportion is a purely a macroscopic parameter and does not consider inter-species differences in olfactory sensory neuron size. Moreover, the parameter should not be confused with other parameters of interest such as discrimination, sensitivity, or acuity. Sensitivity is the ability to sense low concentrations, and is known to relate to the overall number of receptors (Smith and Bhatnagar 2004). Discrimination is the ability to distinguish different odors, and depends on the variety of receptor types or olfactory genes involved. Olfactory acuity is likely a combination of both sensitivity and discrimination, which do not relate to our definition of efficiency.

The mammalian total olfactory surface area is roughly isometric, with an exponent of 0.62 (close to 0.67 as required by isometry). However, all other surface area trends scale with exponents ranging from 0.34 to 0.49 (Fig. 2B and Table 1). The fact that all of these exponents are smaller than 0.67 indicates that moths, representing the smaller animals studied, have proportionally more olfactory sensing area than mammals.

Without such complex 3D structures to pack large surface areas into small volumes, the olfactory system would be ungainly to carry and accrue large aerodynamic drag. In Fig. 3A–C, we show that one antenna of a gypsy moth has a sensilla surface area of 50 mm<sup>2</sup>. The coyote's olfactory epithelium surface area in one nasal fossa is 100 cm<sup>2</sup> (similar to a DVD). One nasal fossa of a human's olfactory epithelium surface area is 5 cm<sup>2</sup>. From this visual representation of moths and mammals,

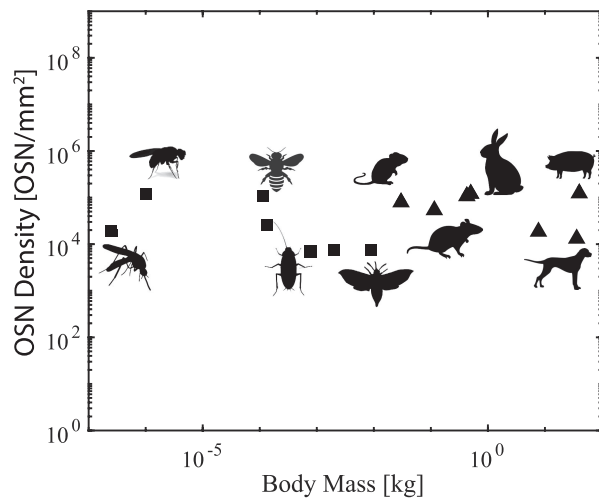


**Fig. 4** Relation between olfactory sensory neuron (OSN) density (OSNs/mm<sup>2</sup>) and body mass  $M$  (kg). Squares represent insect OSN density and triangles represent mammal OSN density. Data for each measurement category was collected from the following literature sources: OSN count (Galizia and Sachse 2010; Breer et al. 2019; Meisami 1989; Kawagishi et al. 2014; Moulton and Beidler 1967; Gasser 1956; Allison and Turner Warwick 1949; Meisami et al. 1990), and OSN density (Horowitz et al. 2014).

it is clear that the proportion of sensing surface area decreases with body size.

Fig. 4 shows the relation between OSN density and body mass for seven insects and seven mammals. Qualitatively, both insects and mammals have a decreasing density of OSNs with increasing body size. Moreover, the density has an upper limit of roughly 120,000 OSNs per mm<sup>2</sup>.

Closely related species might have a similar olfactory surface area due to their closeness rather than due to adaptive reasons. We performed statistical analysis to test the hypothesis that the trends observed are due to phylogenetic closeness (see Methods). We find a  $P$ -value of 0.063 and  $1.37e-08$  for mammalian epithelium (sensing) and turbinates (total) surface area, respectively (Table 1). As the  $P$ -value is less than 0.05 for the total surface area, our hypothesis is supported for the total olfactory surface area of the mammalian species studied. Future researchers might need to add more data points for the total surface area of mammals to draw broader conclusions.

For the moth species examined, we performed statistical analysis to determine if the trend is due to distance from neighboring species using Abouheif's autocorrelation index. We find that moth species mass, sensilla surface area, and total antenna surface area are not correlated with neighboring species (Table 1).

## Discussion

Previous work only established scaling laws for the olfactory sensing surface areas of primates (Smith and Bhatnagar 2004). Here, we expand upon these laws by aggregating additional mammal and moth data. Furthermore, we test previous conclusions that neuronal density is highly variable across closely related species (Collins et al. 2010). Using 14 data points, we find that olfactory sensory neuron density is bounded for both insects and mammals at 120,000 OSNs per mm<sup>2</sup>, although more data will be needed to validate this result. The goal of our presentation of OSN density was to determine order-of-magnitude bounds across species, and to achieve that goal we made a number of assumptions. OSN density is defined as the ratio of the number of neurons to the area observed. The density we presented is only valid for the areas measured by microscopy. In fact, the density may vary with position in the olfactory system. Moreover, previous work that provided OSN numbers supplied a range of values. Instead of reporting a range, we report the average value in that range, again with the goal of achieving order-of-magnitude estimates.

We also give a caveat regarding our measurements of olfactory surface area. For mammals, the surface areas of the olfactory system are estimated using image analysis of CT scan. However, for the moths, we assumed simple geometric shapes such as cylinders for the shape of antenna. Lastly, olfactory neurons themselves vary greatly in their size and in their sensitivity to olfactory molecules. Therefore our measurements of surface area alone cannot be used to determine olfactory acuity.

An important consideration following the discussion of OSN density is the diversity of olfactory receptor (OR) genes. The repertoire of functional OR genes is known to vary extensively among different species, with approximately 1200 functional OR genes in rats, 400 in humans, and 150 in zebrafish (Niimura 2009). The OR repertoire for mammals is encoded by roughly 900–1500 genes, while that of some invertebrates is encoded by only a few hundred genes, including just 60 identified genes in the *Drosophila* (Gaillard et al. 2004). On average, insects have a much smaller OR gene repertoire than mammals, meaning their olfactory capabilities may be more specialized towards particular odors. Therefore, further research that factors in the OSN density per each different receptor is required to compare specificity and sensitivity.

Our analysis of accounting for phylogenetic closeness of the species showed that phylogenetic closeness does play a role in the mammalian total olfactory surface area. As the majority of the species studied were in the *Canidae* family, more diverse range of clades are needed to increase the significance of our scaling law for to-

tal surface area. Moreover, given the greater number of extant moth species compared to that of mammals, the total surface area scaling data could benefit from added phenotypic diversity among insects as well.

In our reporting of the sensing proportion, we assume that sensing and non-sensing surface areas of the olfactory organ are non-intersecting. However, in some animals, this distinction may not be so clear. Warming and humidifying the air are implicated with non-olfactory parts of turbinates, and these parts tend to scale isometrically (Smith et al. 2007). Olfactory zones may have dual functions for both respiration and olfaction. Such dual-function turbinates are more common in shorter-snouted mammals such as cats than long-snouted mammals such as dogs (Pang et al. 2016).

The diversity of olfactory systems becomes even broader if we consider underwater olfaction. Our study focused on olfaction in air; olfaction underwater involves higher fluid density, higher viscosity, and lower diffusion rates of olfactory molecules. Discussions of the underlying physics can be found in recent work on chemical detection of lobsters and crayfish (Koehl et al. 2001; Moore and Crimaldi 2004; Waldrop et al. 2018). In addition, there remain many questions regarding animals that can detect chemical signals in both air and water. Crabs, for example, use the same antennules to sniff in both terrestrial and aquatic environments. Amphibians undergo morphological and physiological changes to the respiratory system as they transition from aquatic to dual aquatic-aerial breathing (Burggren and Infantino 1994). Measurement of their olfactory organs at different stages of transitioning to air breathing may offer additional insight into the evolutionary purpose of the mucus coating on sensing surfaces. In fully developed amphibians, water must be cleared from the nasal passages to allow chemical sensing when the animal transitions from water to air.

## Conclusion

In this work, we presented scaling laws for the surface area and neuron density of the olfactory organs of moths and mammals across nine orders of magnitude in body mass. We showed that the total olfactory surface area is 7-10 times the sensing surface area. The olfactory sensory neuron density had a relatively small range of 10,000 to 100,000 neurons per square mm across the insects and mammals studied. Measuring surface area and neuron density is an important first step in understanding the scaling of olfaction with body size. Understanding olfactory sensitivity and discrimination across body size are difficult interdisciplinary problems that require consideration of olfactory genes and fluid flows. Currently the rate-limiting step in this approach

are the methods of measuring olfactory surface area for diverse species of animals using such CT scanning and LEXT confocal microscopy. We hope that this work will encourage basic research in this topic, which will help identify further unifying perspectives in olfaction.

## Acknowledgments

We thank Tim Smith for sending us his original marmoset data. This material is based upon work supported by the National Science Foundation Graduate Research Fellowship for TS, the National Science Foundation Grant Number 1510884 and Woodruff Faculty Fellowship for DH, and PHEROAERO, funded by the Region Centre Val de Loire for JC.

## Supplementary data

Supplementary data available at *ICB* online.

## References

- Abouheif E. 1999. A method for testing the assumption of phylogenetic independence in comparative data. *Evol Ecol Res* 1:895–09.
- Abrams S. 2019. Rhesus macaque (*Macaca mulatta*). Merrimac, MA 1860, USA, New England Primate Conservancy.
- Allison AC, Turner Warwick RT. 1949. Quantitative observations on the olfactory system of the rabbit. *Brain* 72:186–97.
- Breer H, Fleischer J, Pregitzer P, Krieger J. 2019. Olfactory concepts of insect control – alternative to insecticides. Vol. 2. Springer Nature Switzerland AG, Springer.
- Buck LB. 2000. The molecular architecture of odor and pheromone sensing in mammals. *Cell* 100:611–8.
- Burggren W, Infantino R. 1994. The respiratory transition from water to air breathing during amphibian metamorphosis. *Am Zool* 34:238–46.
- Calder WA. 1996. Size, function, and life history. Dover Publications, Mineola, NY, USA, Courier Corporation.
- Cheer A, Koehl M. 1987. Fluid flow through filtering appendages of insects. *Math Med Biol* 4:185–99.
- Collins CE, Airey DC, Young NA, Leitch DB, Kaas JH. 2010. Neuron densities vary across and within cortical areas in primates. *Proc Natl Acad Sci USA* 107:15927–32.
- Gaillard I, Rouquier S, Giorgi D. 2004. Olfactory receptors. *Cel Mol Life Sci* 61:456–69.
- Galizia C, Sachse S. 2010. The neurobiology of olfaction. London, UK, CRC Press/Taylor & Francis.
- Garman H. 1921. The relation of the kentucky species of solidago to the period of activity of adult cyllene robiniae. Kentucky Agricultural Experiment Station 1. Lexington, KY, USA.
- Gasser HS. 1956. Olfactory nerve fibers. *J Gen Physiol* 39:473–96.
- Green PA, Van Valkenburgh B, Pang B, Bird D, Rowe T, Curtis A. 2012. Respiratory and olfactory turbinal size in canid and arctoid carnivorans. *J Anat* 221:609–21.
- Gross EA, Swenberg JA, Fields S, Popp JA. 1982. Comparative morphometry of the nasal cavity in rats and mice. *J Anat* 135:83–8.

- Grosmaître X, Santarelli LC, Tan J, Luo M, Ma M. 2007. Dual functions of mammalian olfactory sensory neurons as odor detectors and mechanical sensors. *Nat Neurosci* 10:348–54.
- Hedberg K. 2007. Developing a relevant weight for age chart for Australian GSDs. Mt. Barker SA 5251, German Shepherd Dog Council of Australia.
- Howland HC, Merola S, Basarab JR. 2004. The allometry and scaling of the size of vertebrate eyes. *Vision Res* 44:2043–65.
- Horowitz LF, Saraiva LR, Kuang D, Yoon KH, Buck LB. 2014. Olfactory receptor patterning in a higher primate. *J Neurosci* 34:12241–52.
- Jacob V, Scolari F, Delatte H, Gasperi G, Jacquin-Joly E, Malacrida AR, Duyck PF. 2017. Current source density mapping of antennal sensory selectivity reveals conserved olfactory systems between tephritids and *Drosophila*. *Scient Rep* 7:15304.
- Jumbo-Lucioni P, Ayroles JF, Chambers MM, Jordan KW, Leips J, Mackay TFC, De Luca M. 2010. Systems genetics analysis of body weight and energy metabolism traits in *Drosophila melanogaster*. *BMC Genomics* 11:297.
- Kandel ER, Schwartz JH, Jessell TM. 2000. Principles of neural science. Vol. 4. New York (NY): McGraw-Hill.
- Kawagishi K, Ando M, Yokouchi K, Sumitomo N, Karasawa M, Fukushima N, Moriizumi T. 2014. Stereological quantification of olfactory receptor neurons in mice. *Neuroscience* 272:29–33.
- Meisami E, Louie J, Hudson R, Distel H. 1990. A morphometric comparison of the olfactory epithelium of newborn and weanling rabbits. *Brain* 72:186–97.
- Kobayashi E, Hishikawa S, Teratani T, Lefor AT. 2012. The pig as a model for translational research: overview of porcine animal models at Jichi Medical University. *Transplant Res* 1:1.
- Koehl MAR, Koseff JR, Crimaldi JP, McCay MG, Cooper T, Wiley MB, Moore PA. 2001. Lobster sniffing: antennule design and hydrodynamic filtering of information in an odor plume. *Science* 294:1948–51.
- Koella JC, Lyimo EO. 1996. Variability in the relationship between weight and wing length of *Anopheles gambiae* (diptera: Culicidae). *J Med Entomol* 33:261–4.
- Lindsey R. 2002. Locust! Earth Observatory. Accessed March 25, 2022, <https://earthobservatory.nasa.gov/features/Locusts>.
- Lockey JK, Willis MA. 2015. One antenna, two antennae, big antennae, small: total antennae length, not bilateral symmetry, predicts odor-tracking performance in the American cockroach *Periplaneta americana*. *J Experim Biol* 218:2156–65.
- Martins EP, Hansen TF. 1997. Phylogenies and the comparative method: a general approach to incorporating phylogenetic information into the analysis of interspecific data. *Am Natur* 149:646–67.
- McEwen DP, Jenkins PM, Martens JR. 2008. Olfactory cilia: our direct neuronal connection to the external world. *Curr top Developm Biol* 85:333–70.
- Meisami E. 1989. A proposed relationship between increases in the number of olfactory receptor neurons, convergence ratio and sensitivity in the developing rat. *Develop Brain Res* 46:9–19.
- Moore P, Crimaldi J. 2004. Odor landscapes and animal behavior: tracking odor plumes in different physical worlds. *J Marine Syst* 49:55–64.
- Mongeau JM, Sponberg SN, Miller JP, Full RJ. 2015. Sensory processing within cockroach antenna enables rapid implementation of feedback control for high-speed running maneuvers. *J Experim Biol* 218:2344–54.
- Moulton DG, Beidler LM. 1967. Structure and function in the peripheral olfactory system. *Physiol Rev* 47:1.
- Münkemüller T, Lavergne S, Bzeznik B, Dray S, Jombart T, Schiffrers K, Thuiller W. 2012. How to measure and test phylogenetic signal. *Meth Ecol Evol* 3:743–56.
- Nijhout H, Davidowitz G, Roff D. 2006. A quantitative analysis of the mechanism that controls body size in *Manduca sexta*. *J Biol* 5:3615–20.
- Nijland R, Burgess JG. 2010. Bacterial olfaction. *Biotechnol J* 5:974–77.
- Nimura Y. 2009. Evolutionary dynamics of olfactory receptor genes in chordates: interaction between environments and genomic contents. *Human Genomics* 4:107.
- Nummela S. 1995. Scaling of the mammalian middle ear. *Hearing Res* 85:18–30.
- Pang B, Yee KK, Lischka FW, Rawson NE, Haskins ME, Wysocki CJ, Craven BA, Van Valkenburgh B. 2016. The influence of nasal airflow on respiratory and olfactory epithelial distribution in felids. *J Experim Biol* 219:1866–74.
- Pavoine S, Ollier S, Pontier D, Chessel D. 2008. Testing for phylogenetic signal in phenotypic traits: new matrices of phylogenetic proximities. *Theoret Popul Biol* 73:79–91.
- Purves D, Augustine GJ, Fitzpatrick D, Katz LC, LaMantia AS, McNamara JO, Williams SM. 2001. 337–366. *Neuroscience*. 2nd ed. Sunderland (MA): Sinauer Associates.
- Saager F, Gewecke M. 1989. Antennal reflexes in the desert locust *Schistocerca gregaria*. *J Experim Biol* 147:519–32.
- Sachse S, Krieger J. 2011. Olfaction in insects. *e-Neuroforum* 2:49.
- Saltin BD, Matsumura Y, Reid A, Windmill JF, Gorb SN, Jackson JC. 2019. Material stiffness variation in mosquito antennae. *J Royal Soc Interface* 16:1–10.
- Sankaran S, Khot LR, Panigrahi S. 2012. Biology and applications of olfactory sensing system: a review. *Sens Actuators B: Chem* 171:1–17.
- Schmidt-Nielsen K, Knut SN. 1984. *Scaling: why is animal size so important?*. Cambridge, England, UK, Cambridge University Press.
- Schneider CA, Rasband WS, Eliceiri KW. 2012. NIH Image to ImageJ: 25 years of image analysis. *Nat Meth* 9:671.
- Shields VDC, Hildebrand JG. 2001. Recent advances in insect olfaction, specifically regarding the morphology and sensory physiology of antennal sensilla of the female sphinx moth *Manduca sexta*. *Microsc Res Tech* 55:307–29.
- Smith T, Bhatnagar K. 2004. Microsmatic primates: Reconsidering how and when size matters. *Anat Rec* 279B:24–31.
- Smith TD, Bhatnagar KP. 2004. Microsmatic primates: Reconsidering how and when size matters. *Anat Rec* 279B:24–31.
- Smith TD, Bhatnagar KP, Rossie JB, Docherty BA, Burrows AM, Cooper GM, Mooney MP, Siegel MI. 2007. Scaling of the first ethmoturbinal in nocturnal strepsirrhines: olfactory and respiratory surfaces. *Anat Rec* 290:215–37.
- Smith TD, Eiting TP, Rossie JB. 2011. Distribution of olfactory and nonolfactory surface area in the nasal fossa of *Micro-*

- cebus murinus*: implications for microcomputed tomography and airflow studies. *Anat Rec* 294:1217–25.
- Smith TD, Eiting TP, Bonar CJ, Craven BA. 2014. Nasal morphometry in marmosets: loss and redistribution of olfactory surface area. *Anat Rec* 297:2093–104.
- Spencer TL, Mohebbi N, Jin G, Forister ML, Alexeev A, Hu DL. 2020. Moth-inspired methods for particle capture on a cylinder. *J Fluid Mech* 884:A34.
- Spencer T, Clark A, Fonollosa J, Virost E, Hu D. 2021. Sniffing speeds up chemical detection by controlling airflows near sensors. *Nat Commun.*12:1–10.
- Symonds MR, Johnson TL, Elgar MA. 2012. Pheromone production, male abundance, body size, and the evolution of elaborate antennae in moths. *Ecol Evol* 2:227–46.
- Tsujiuchi S, Sivan-Loukianova E, Eberl DF, Kitagawa Y, Kawawaki T. 2007. Dynamic range compression in the honey bee auditory system toward waggle dance sounds. *PLoS One* 2:2.
- Vršanský P, Wang B. 2017. A new cockroach, with bipectinate antennae (blattaria: Olidae fam. nov.), further highlights the differences between the burmite and other faunas. *Biologia* 72:1327–33.
- Waldrop LD, He Y, Khatri S. 2018. What can computational modeling tell us about the diversity of odor-capture structures in the pancrustacea? *J Chem Ecol* 44: 1084–100.
- Wyatt TD. 2009. Fifty years of pheromones. *Nature* 457: 262–3.
- Xi J, Si XA, Kim J, Zhang Y, Jacob RE, Kabilan S, Corley RA. 2016. Anatomical details of the rabbit nasal passages and their implications in breathing, air conditioning, and olfaction. *Anat Rec* 299:853–68.
- Yee KK, Craven BA, Wysocki CJ, Van Valkenburgh B. 2016. Comparative morphology and histology of the nasal fossa in four mammals: gray squirrel, bobcat, coyote, and white-tailed deer. *Anat Rec* 299:840–52.
- Żółtowska K, Fraczek R, Lipiński Z. 2011. Hydrolases of developing worker brood and newly emerged worker of *Apis mellifera carnica*. *J Apicul Sci* 55:27–37.